

## Bias-controlled friction of InAs nanowires on a silicon nitride layer studied by atomic force microscopy

G. Conache,<sup>1,2</sup> A. Ribayrol,<sup>1</sup> L. E. Fröberg,<sup>1</sup> M. T. Borgström,<sup>1</sup> L. Samuelson,<sup>1</sup> L. Montelius,<sup>1</sup>  
H. Pettersson,<sup>1,2</sup> and S. M. Gray<sup>1</sup>

<sup>1</sup>*Solid State Physics and the Nanometer Structure Consortium, Lund University, P.O. Box 118, SE-22100 Lund, Sweden*

<sup>2</sup>*Center for Applied Mathematics and Physics, Halmstad University, P.O. Box 823, SE-301 18 Halmstad, Sweden*

(Received 21 April 2010; published 2 July 2010)

By studying how nanowires lying on a surface bend when pushed by an atomic force microscopy tip we are able to measure the friction between them and the substrate. Here, we show how the friction between InAs nanowires and an insulating silicon nitride layer varies when a dc voltage is applied to the tip during manipulation. The bias charges the capacitor formed by the wire and the grounded silicon back contact. Electrostatic forces increase the contact pressure and allow us to tune the friction between the wire and the silicon nitride surface. Using nanowires of about 40–70 nm diameter and a few microns in length we have applied biases in the range +12 to –12 V. A monotonic increase of the sliding friction with voltage was observed. This increase in friction with the normal force implies that the mesoscopic nanowire-surface system behaves like a macroscopic contact, despite the nanometer size of the contact in the direction of motion. The demonstrated bias-controlled friction has potential applications in MEMS/NEMS devices.

DOI: [10.1103/PhysRevB.82.035403](https://doi.org/10.1103/PhysRevB.82.035403)

PACS number(s): 62.20.Qp, 62.23.Hj

### I. INTRODUCTION

Friction is a fascinating subject that has been studied on many different length scales, starting with the macroscopic friction laws of Amontons and Coulomb and, after the invention of the friction force microscope, at the nanometer-scale and at the atomic level.<sup>1–3</sup>

In the process of miniaturization of tools such as magnetic storage and MEMS/NEMS devices, friction is of crucial importance since it strongly affects the devices' performance and sometimes prevents them from operating.<sup>4,5</sup> Thus there is a need to study friction on the mesoscopic length scale, to bridge the gap between macroscopic friction and atomic scale friction not only from a fundamental science point-of-view, but also for the purpose of applications.<sup>3</sup>

A theory of electronic contributions to friction has been proposed by Persson, considering the motion of small particles on a conducting film, and linking the change in resistivity to electron-hole pair damping.<sup>6</sup> One possible example was demonstrated by Park *et al.*, using a conductive atomic force microscopy (AFM) tip scanning on Si *p-n* junctions, where excess friction was observed in the highly doped *p*-regions.<sup>7,8</sup> More recently, a similar excess friction was observed on *n*-type GaAs.<sup>9</sup>

In both cases at least some of the increase in friction with voltage originates from electrostatic effects modifying the normal forces between the tip and substrate. Thus, even in the absence of friction caused by new fundamental loss mechanisms, it seems possible to control friction with an electronic signal, which is of great technological interest.

We have previously developed a technique that allows us to measure friction on the mesoscopic scale.<sup>10,11</sup> It uses AFM-based manipulation to bend the nanowires or translate them across the surface. The curvature of the wire after manipulation is determined by a balance between friction with the substrate and elastic strain in the wire. We have shown that both static and sliding friction forces may be measured by a suitable choice of manipulation.

In Ref. 11 we presented data on the friction force per unit length versus the diameter of nanowires deposited on silicon nitride layers on silicon substrates. An increase in the static friction with the diameter was observed that could not be explained using simple models. At the same time, sliding friction did not vary significantly with the diameter, provided the wires were sufficiently thick—above around 40 nm in diameter. Thinner wires experience stick-slip motion instead of true sliding.

Although we have established clear patterns of tribological behavior for these nanowires, it is not obvious which of the classic friction parameters are contributing to or dominating that behavior. In particular, the variation of friction with normal force can only be studied indirectly, by making assumptions about how the van der Waals force holding the nanowire onto the substrate varies with diameter. In the work presented here, we have varied the normal force for individual nanowires by applying a dc bias with a conductive AFM tip. The AFM tip charges the capacitor formed by the wire and substrate and the contact pressure between the two increases because of the resultant attractive Coulomb forces.

### II. EXPERIMENTAL DETAILS

All friction measurements in this work were performed on InAs nanowires fabricated by chemical beam epitaxy (CBE). Full details of the growth procedure are given in Ref. 12. Briefly, size-selected gold particles were produced with an aerosol method,<sup>13</sup> and deposited on an InAs (111)B substrate. After transfer to a CBE growth chamber the substrate oxide was removed by heating under an As pressure. Growth was performed using trimethylindium (TMIn) and precracked tertiarybutylarsine (TBAs). The nanowires exhibit wurtzite crystal structure, have hexagonal cross sections with diameters in the range 40–70 nm, and are 3–4  $\mu\text{m}$  long. ‘Diameter’ in this paper refers to the distance between opposite parallel side facets of the nanowire.

The InP nanowires used for the comparative study of charging were grown by low-pressure (100 mbar) metalorganic vapor phase epitaxy (MOVPE) and contained *pn* junctions. The Au aerosol particles were deposited on a (111)B InP substrate. Trimethylindium (TMIn), phosphine (PH<sub>3</sub>), dimethylzinc (DMZn) (for the *p*-doping) and tetraethylthi (TESn) (for the *n*-doping) were used as precursors with hydrogen (H<sub>2</sub>) as carrier gas using HCl as an *in situ* etching agent to eliminate tapering. Full details of the growth are given elsewhere.<sup>14,15</sup>

The 1–10 Ω cm substrates used for our friction experiments were phosphorous doped *n*-type silicon with a 120 nm coating of silicon nitride deposited by plasma enhanced chemical vapor deposition (PECVD). The substrates were patterned with gold dots and location markers using e-beam lithography to allow us identify and revisit individual nanowires. Nanowires were transferred to the substrates using a piece of clean room wipe in a dry “wipe-on, wipe-off” method. SEM and AFM confirm that although wire bundles do form, isolated single wires can easily be found, and they lie on a substrate with one facet of the hexagonal prism in contact with the surface.<sup>10,11</sup>

We used rectangular Si AFM cantilevers with a nominal spring constant of the order of 30–40 N/m, coated with a layer of Pt/Ir on the tip and on the cantilever. The experiments were carried out in an ISO Class 5 clean room, in which the temperature and humidity are controlled to 17 ± 0.5 °C and 24 ± 3%, respectively.

The nanowire was pushed using the ‘retrace lift’ mode of our Nanoscope IIIa Dimension 3100 AFM from Veeco. The manipulation procedure has been described in detail in Refs. 10 and 11. We disable the slow scan axis where we want to apply the manipulation force so that the tip scans back and forth along the same line during the manipulation. A conventional tapping mode contour is acquired on the forward scan while the oscillation of the cantilever is quenched on the backward scan and the AFM feedback loop is turned off. The tip retraces the contour measured on the forward scan, but with an offset force applied so that the tip moves toward the surface. The offset force is increased in small steps until the desired movement of the nanowire is observed as a shift in the trace signal.

Sliding friction is measured by pushing the wire in the middle, perpendicular to its long axis. Friction bends the wire back behind the tip as it is pushed across the surface with a constant shape, with all parts of the nanowire moving at the same velocity. The scanning speed of the tip during manipulation was about 3 μm/s in all experiments.

For bias-dependent manipulation a voltage was applied to the tip only during the retrace scan. At all other times the tip was grounded, thus allowing accurate measurements of the wire during the trace scan and in subsequent imaging.

The friction force per unit length was determined from the radius of curvature of the bent NW after manipulation.<sup>10,11</sup> The radius of curvature is calculated using software that traces the backbone of the wire, avoiding artifacts from tip-sample convolution. The friction force per unit length is given in convenient units by

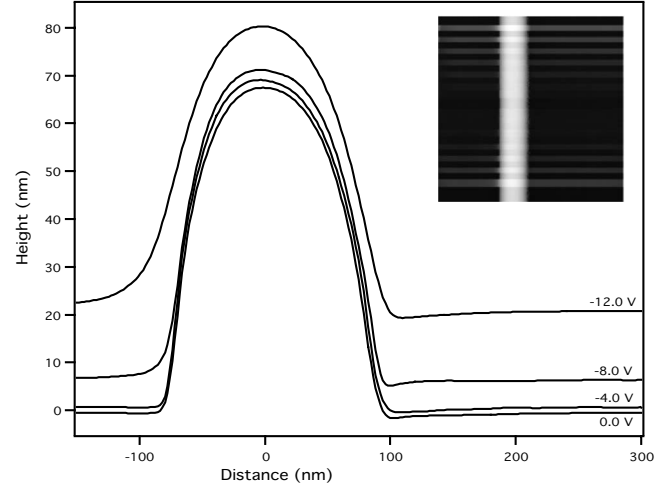


FIG. 1. Voltage-dependent tapping mode line scans across a 68 nm InAs nanowire on Si<sub>3</sub>N<sub>4</sub>. The inset shows the full data set as an image, illustrating how the apparent height changes abruptly each time the bias changes. From top to bottom, the bias in each strip of approximately 15 lines is 0, -12, 1, -11, 2, -10, 3, -9, 4, -8, 5, -7, 6, 0, -6, 7, -5, 8, -4, 9, -3, 10, -2, 11, -1, 12, and 0 V. The main graph shows four individual line scans at increasingly negative biases, averaged over the relevant strip of the image.

$$\frac{F}{(\text{pN/nm})} = \frac{5000\sqrt{3}}{288} \frac{E}{\text{GPa}} \frac{(D/\text{nm})^4}{(R/\text{nm})^3} \quad (1)$$

where  $E$  is the Young’s modulus in GPa,  $D$  is the diameter of the wire in nm, and  $R$  is the radius of curvature at the most tightly bent part of the wire, also in nm. For the Young’s modulus we used values obtained from a linear fit to the experimental values for similar InAs nanowires published by Lexholm *et al.*<sup>16</sup>

### III. RESULTS AND DISCUSSION

In principle, many effects can influence the charging of the combined nanowire-substrate system. The total capacitance will have components from the intrinsic capacitance-voltage characteristic of the nanowire, and also from space charge effects and band bending in the silicon support wafer. The rate of charge transfer is most likely limited by tunneling of charge through the native oxide on the nanowire, which for bulk InAs is typically 1–2 nm thick.<sup>17,18</sup>

For reproducible friction data the most important factor is to ensure that the wire is fully charged when in motion. To this end we measured the effect of nanowire charging on the AFM’s operation, and confirmed that the wire charges sufficiently rapidly.

Figure 1 shows a series of tapping mode AFM line scans performed across the axis of a 68 nm thick InAs nanowire on a 120 nm Si<sub>3</sub>N<sub>4</sub> layer, with the slow-scan axis disabled so that the same section of the wire is scanned repeatedly. The inset image shows how the apparent height of the nanowire and the substrate both change as a sequence of dc voltages is applied to the tip. We alternate the voltage between positive and negative values so as to ensure a clear transition between

successive bias levels. Heights are referenced to a plane fitted to the substrate portions of zero bias strips measured at the bottom, center and top of the image. This allows us to correct for vertical drift and any lateral tilt of the surface. Lateral drift, if observed, is corrected by shifting line scans so that the profile of the nanowire forms a bright vertical line in the image.

The individual scans within a strip can be averaged for better signal to noise, and four such average contours can be seen in the main plot of Fig. 1. In general, the variation of height with voltage can be complex, as MIS-like band bending in the semiconducting support wafer, and the voltage-capacitance characteristics of the nanowire itself change the amounts and spatial distributions of any stored charge, and hence the observed forces. A full description of the height changes seen on the substrate and the wire is beyond the scope of this paper and will be presented elsewhere. What is immediately clear however, is that the apparent height and width of the wire both change as the bias on the AFM tip increases, and that the height changes are different from those seen on the substrate. In the simplest model, the biased tip experiences two electrostatic forces: a Coulomb repulsion from charge transferred onto the nanowire, and an attraction to image charges in the conducting silicon substrate. As expected, we observe a smaller height change over the wire than over the bare surface, as the first mechanism only applies in the vicinity of the wire.

It is important to stress that these are tapping mode height contours. Long-range electrostatic forces do not affect a measured height directly, but lead to an additional suppression of the cantilever's tapping mode oscillation. The AFM feedback loop retracts the cantilever to compensate, which leads to an apparent height change. Despite this indirect measurement, the great advantage of working in tapping mode is that mechanical interactions between the tip and the nanowire and substrate are minimized.

Figure 2 shows the height changes on the apex of two different nanowires as the bias is changed. The top trace is for a second 68 nm InAs nanowire, and is equivalent to a vertical section along the apex of the bright stripe in the line scan image. The flat sections for each individual bias are good evidence that the nanowire, and the silicon substrate charge quickly compared to the time scales relevant to our experiments. This is not always the case. A counter example is given by the lower trace, from a 40 nm InP nanowire lying on a 330 nm SiO<sub>2</sub> layer on an identical silicon substrate. Here, clear charging transients are observed with time constants of the order of 10 s. This particular wire was doped so as to have a *p-n* junction half way along its length. Similar charging transients were observed on both *p*-type and *n*-type sections of the wire, and for both bias polarities, indicating that charge injection was generally inefficient compared to the InAs wire. Our experience is that it is important to check for charging transients before conducting bias-dependent friction measurements on a new class of nanowire or substrate.

We have not observed any such charging transients for the InAs nanowires used for our friction experiments, and we can be sure that charging must be sufficiently fast that any transients take place on a single scan line. We can thus esti-

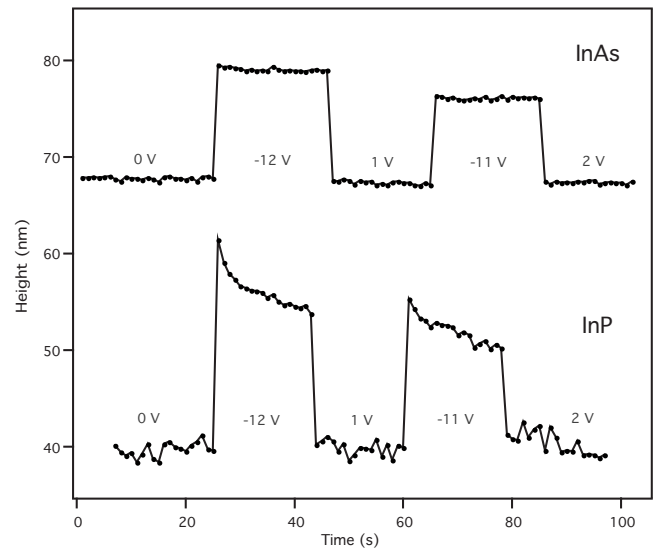


FIG. 2. Variations in the apparent height of two nanowires as the tip bias is changed between the values shown. The upper trace is from a 68 nm InAs nanowire on Si<sub>3</sub>N<sub>4</sub>. The lower curve is from an *n*-type section of a 40 nm InP nanowire on SiO<sub>2</sub>. The InP wire shows clear charging transients as the bias is switched to negative values.

mate the time needed to charge the nanowire during manipulation, taking into account that the tip is only in intermittent contact with the surface in tapping mode. Measurements of the actual current flow in biased-tip tapping mode AFM on metals indicate that the short-range nature of charge injection, via tunneling or direct conduction, limit it to around 2% of the oscillation cycle.<sup>19,20</sup> Thus charge transfer in our manipulation experiments can be expected to be 50 times faster than in tapping mode, which corresponds to less than one pixel of a typical image, or a distance of 10 nm. We usually push wires for at least a few hundred nanometers at each step of a friction experiment, and so we can be confident that they slide fully charged, and that they are rapidly discharged during the postmanipulation imaging, which allows for high resolution measurements.

Figure 3 shows a typical friction experiment on an InAs nanowire on a silicon nitride/silicon substrate. Note that in this case, the bias is only applied on the retrace scan during the actual manipulation, and all other imaging takes place at zero bias. An arrow in each image shows how and where the nanowire was pushed, while the applied voltage for a particular push is indicated between the images. Figure 3(a) shows the starting configuration of the nanowire, which was then pushed at its center with 0 V applied to the tip. Figure 3(b) shows that the manipulation resulted in a slightly bent wire. Next the wire was pushed with +5 V on the tip resulting in a more strongly bent wire as seen in Fig. 3(c). The extra bending is a sign that the friction with the substrate has increased. Pushing it again at +5 V results in a wire with approximately the same curvature [Fig. 3(d)], showing that the friction is maintained at the new, higher level. Most importantly, a further push with the bias returned to 0 V reduces the curvature again [Fig. 3(e)], showing that the increase in friction with bias is reversible. The actual values of the fric-

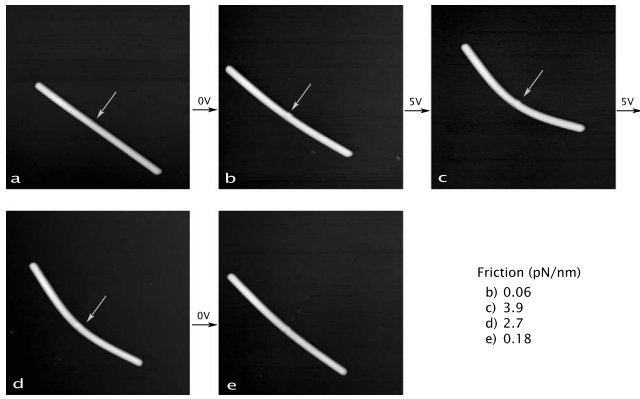


FIG. 3. Voltage-dependent manipulation of a 51 nm diameter InAs nanowire on Si<sub>3</sub>N<sub>4</sub>. The arrows in the images show the position and direction of the push applied with the AFM tip. The tip bias was 0 V for the push from (a) to (b), then +5, +5, and 0 V between subsequent images. The sliding friction calculated from the curvature of the wire for each image is also shown.

tion force per unit length calculated for the nanowire after each manipulation step are also given in the figure.

In Fig. 4 we plot the friction per unit length versus bias for a 48 nm InAs nanowire. The manipulation steps in this case were performed at 0, +5, +7, and +9 V and the wire displays a typical behavior with a smooth monotonic increase in friction with voltage. Subsequently, the wire was pushed at a negative voltage of -9 V, again resulting in a high friction, and consistent with a symmetrical variation of the friction with bias. Finally, the voltage was returned to zero, and although the friction reduced from its high value, it remained higher than had been the case before any voltage was applied. We ascribe this hysteresis to charging of trap states in the native oxide layer on the nanowire. The trapped

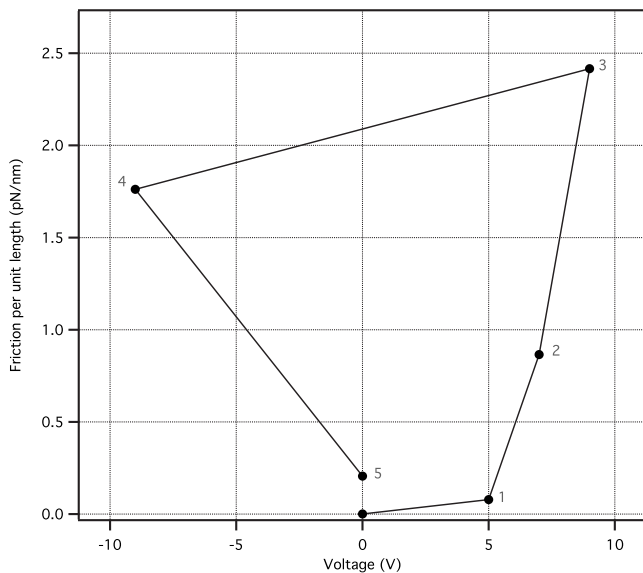


FIG. 4. Plot of the friction per unit length vs tip bias for a 48 nm InAs nanowire on a Si<sub>3</sub>N<sub>4</sub> substrate. The sequence of pushes is indicated by the numbers beside each data point.

charge experiences a Coulomb force even after the bulk of the wire has returned to ground potential, and so maintains a raised level of friction.

Although the pattern of behavior seen in Fig. 4 is repeatable, we have observed a strong variability in the magnitude of the friction increase. Some wires such as the one in Fig. 4 show an increase of the order of 3000, while others show only a modest increase of a factor less than 10. From measurements such as those shown in Figs. 1 and 2 we can be confident that this variability is not due to insufficient charging. We also do not believe that the largest relative increases are due to a transition to stick-slip friction, as we have seen for small diameter wires at zero bias,<sup>11</sup> which would be one way to dramatically increase the apparent magnitude of sliding friction, but which would be expected to show a threshold behavior rather than the smooth increase with voltage seen here. The insulating silicon nitride layer is sufficiently thick that we can also rule out variations in the structure or thickness of the 1–2 nm of native oxide causing dramatic changes to the electrostatic forces between the wire and the substrate.

It seems more likely that trap states in the silicon nitride layer are changing the electrostatic fields in such a way as to reduce the magnitude of the induced attraction between the wire and substrate. We have in one experiment observed surface charging, seen as a trail of raised height behind the moving wire that slowly decays in subsequent images. It is possible that such charging occurs to a lesser extent with all our wires. Charge transfer to a surface trap state will take place by tunneling from the wire through the native oxide to the trap, and here, small changes in the thickness or composition of the native oxide can strongly affect trap occupation statistics, and so lead to a large variability in the observed friction increase. It would be useful to conduct experiments with a less thick insulating layer and a more conductive substrate wafer in order to allow the use of smaller voltages, thus reducing electronic interactions with trap states.

The symmetric behavior with bias is to be expected from the polarity-independent attractive Coulomb forces, between the nanowire and the substrate. It is tempting to fit a parabola to the data points, assign a constant capacitance, and apply the well-known result that the force on the electrodes of a capacitor depends upon the voltage squared. The increase in friction seen here would then be linear in the induced normal force and we would have recovered Amontons' Law. Unfortunately, we know from the charging experiments that the capacitance of these wires cannot be constant, as is well established by direct measurements of the gate capacitance of nanowire FETs in a wrap-gate configuration.<sup>21,22</sup> It is also worth remarking that the increase in friction with voltage is usually stronger than parabolic. Detailed modeling of the charge distributions in the wire and substrate will be necessary for a full quantitative understanding of these effects.

IV. CONCLUSIONS

We have demonstrated that the sliding friction of InAs nanowires on a silicon nitride surface can be electrically

tuned by a dc bias applied to the AFM tip during manipulation. A reversible, monotonic increase of up to three orders of magnitude in the sliding friction with the voltage was observed. Some hysteresis occurred, with a remanent friction persisting after high voltages had been applied, which we ascribe to filling of trap states in the native oxide coating the nanowire. The increase in friction with increasing normal force suggests that these nanowires behave more like macro-

scopic objects than atomic-scale point contacts.

#### ACKNOWLEDGMENTS

The authors acknowledge financial support from the European Commission (6th Framework Program Grant No. NMP4-CT-2005-017071), the Swedish Research Council and the Swedish Foundation for Strategic Research.

- 
- <sup>1</sup>C. M. Mate, G. M. McClelland, R. Erlandsson, and S. Chiang, *Phys. Rev. Lett.* **59**, 1942 (1987).  
<sup>2</sup>J. Krim, *Surf. Sci.* **500**, 741 (2002).  
<sup>3</sup>I. Szlufarska, M. Chandross, and R. W. Carpick, *J. Phys. D* **41**, 123001 (2008).  
<sup>4</sup>R. Maboudian and R. T. Howe, *J. Vac. Sci. Technol. B* **15**, 1 (1997).  
<sup>5</sup>B. Bhushan, *Handbook of Micro/Nanotribology*, 2nd ed. (CRC Press LLC, USA, 1999).  
<sup>6</sup>B. N. J. Persson, *Phys. Rev. B* **44**, 3277 (1991).  
<sup>7</sup>J. Y. Park, Y. Qi, D. F. Ogletree, P. A. Thiel, and M. Salmeron, *Phys. Rev. B* **76**, 064108 (2007).  
<sup>8</sup>J. Y. Park, D. F. Ogletree, P. A. Thiel, and M. Salmeron, *Science* **313**, 186 (2006).  
<sup>9</sup>Y. Qi, J. Y. Park, B. L. M. Hendriksen, D. F. Ogletree, and M. Salmeron, *Phys. Rev. B* **77**, 184105 (2008).  
<sup>10</sup>M. Bordag, A. Ribayrol, G. Conache, L. E. Fröberg, S. Gray, L. Samuelson, L. Montelius, and H. Pettersson, *Small* **3**, 1398 (2007).  
<sup>11</sup>G. Conache, S. M. Gray, A. Ribayrol, L. E. Fröberg, L. Samuelson, H. Pettersson, and L. Montelius, *Small* **5**, 203 (2009).  
<sup>12</sup>M. T. Björk, B. J. Ohlsson, T. Sass, A. I. Persson, C. Thelander, M. H. Magnusson, K. Deppert, L. R. Wallenberg, and L. Samuelson, *Appl. Phys. Lett.* **80**, 1058 (2002).  
<sup>13</sup>M. H. Magnusson, K. Deppert, J.-O. Malm, J.-O. Bovin, and L. Samuelson, *J. Nanopart. Res.* **1**, 243 (1999).  
<sup>14</sup>M. T. Borgström, E. Norberg, P. Wickert, H. A. Nilsson, J. Trägårdh, K. A. Dick, G. Statkute, P. Ramvall, K. Deppert, and L. Samuelson, *Nanotechnology* **19**, 445602 (2008).  
<sup>15</sup>M. T. Borgström, J. Wallentin, J. Trägårdh, P. Ramvall, M. Ek, L. R. Wallenberg, L. Samuelson, and K. Deppert, *Nano Res.* **3**, 264 (2010).  
<sup>16</sup>M. Lexholm, I. Karlsson, F. Boxberg, and D. Hessman, *Appl. Phys. Lett.* **95**, 113103 (2009).  
<sup>17</sup>G. Hollinger, R. Skheyta-Kabbani, and M. Gendry, *Phys. Rev. B* **49**, 11159 (1994).  
<sup>18</sup>D. Y. Petrovykh, M. J. Yang, and L. J. Whitman, *Surf. Sci.* **523**, 231 (2003).  
<sup>19</sup>A. Fein, Y. Zhao, C. A. Peterson, G. E. Jabbour, and D. Sarid, *Appl. Phys. Lett.* **79**, 3935 (2001).  
<sup>20</sup>D. Sarid, *Comput. Mater. Sci.* **5**, 291 (1996).  
<sup>21</sup>S. Roddaro, K. Nilsson, G. Astromskas, L. Samuelson, L.-E. Wernersson, O. Karlström, and A. Wacker, *Appl. Phys. Lett.* **92**, 253509 (2008).  
<sup>22</sup>O. Karlström, A. Wacker, K. Nilsson, G. Astromskas, S. Roddaro, L. Samuelson, and L.-E. Wernersson, *Nanotechnology* **19**, 435201 (2008).